J. Mater. Environ. Sci. 6 (11) (2015) 3217-3225
ISSN : 2028-2508
CODEN: JMESCN

New composite materials based on biosourced polyurethane: Elaboration and study of their thermal and mechanical properties

Fouad MALEK[1*], Stéphane GIRAUD[2], Philippe VROMAN[2] , Jalal ISAAD[3*]

[1]*Laboratory of Organic, Macromolecular Chemistry and Natural Products - URAC 25 - Faculty of Sciences, Mohamed 1st University, Oujda 60000, Morocco.*

[2]*ENSAIT, GEMTEX, F-59100 Roubaix, France*

[3]*Faculty of Technical Sciences of Al Hoceima. Mohamed 1st University, Oujda 60000, Morocco*

Received 25 Jul 2015, Revised 17 Nov 2015, Accepted 27 Nov 2015
** Corresponding Author: Email: fouad_malek@yahoo.fr , Tel : (+212 5 36 50 06 01), (Fouad Malek); jisaadjalal@gmail.com, Tel: (+212 5 36 50 06 01) (Jalal Isaad);*

Abstract

Polyurethane (PU) based on castor oil, 4.4'diphenyl methylene diisocyanate and 1,3-propane diol was synthesized in two-steps. The composites were obtained by blending the PU with various amounts of cellulosic fibers extracted from the Moroccan Alfa stems (esparto grass plant). The influence of the cellulosic fiber ratio on the thermal and mechanical properties of the composites was demonstrated by means of several characterization techniques, such as thermal, mechanical, structural, and morphological analyses. The hydrogen bonding interaction and the possible formation of urethane bonds between PU and the hydroxyl groups of the cellulose provides a good fiber-matrix interface. The variation of glass transition temperature, *Tg*, versus cellulose content is linear. However, the mechanical properties increased up to 20 *wt* % of fibers and decreased beyond this value.

Keywords: Composites, Polyurethane, Cellulose fibers, thermal properties, mechanical properties

Introduction

Due to their potential to replace the petrochemical derivatives in the preparation of the polymeric materials, the use of renewable raw material resources has attracted the attention of many researchers [1-6]. The general interests consist in: (i) the reduction of the fossil fuels dependence, which are rapidly being exhausted [2-4], and (ii) to develop innovative technologies and competitive industrial products.

Vegetable oils, as polyols, are excellent renewable sources of raw materials to manufacture polyurethane (PU) components. They are abundant and relatively cheap renewable resources. They represent a major potential alternative source of chemicals that are suitable for the developing of safe and environmentally eco-friendly products. Natural oils are generally triglyceride esters. Those are comprised of three fatty acids bonded by a glycerol unit. Castor oil is natural oil which is increasingly used in different industries as an alternative to hydrocarbon-based feedstock. It is obtained by extracting or pressing the seed of a plant called "*Ricinus communis*", in the family Eurphorbiacae [7]. Recently, the *castor oil* was used in the preparation of the PU [2, 8-11], and 90% of the fatty acids in the castor oil are the ricinoleic acid (monounsaturated, 18-carbon), which has a hydroxyl functional group at the twelfth carbon. This is a very uncommon property for a biological fatty acid and is the main driving point for the direct use of this oil as a hydroxyl-containing trifunctional monomer.

The *castor oil* also has other advantages such as renewability, easy availability in a large quantity, environmental friendliness, biodegradability, and overall low cost. On the other hand, the use of the natural fibres, for example flax [12, 13], hemp [14], sisal [15, 16], wheat straw [17], ramie [18] and date palm tree [19] can lead to materials with properties such as thermal and impact resistance, low density, flexibility and biodegradability. However, the ensuing properties of the composites depend on many factors like fibre-matrix adhesion, volume fraction of fiber, fiber orientation and polymer uses [20, 21].

The oriental region of Morocco is rich in Alfa plants. This xerophilous plant belongs to the family of grasses and grows to a maximal length of 1 m as cylindrical rods. The esparto is constituted of strong and tenacious stems, as its Latin name "stipa tenacissima'' means. Indeed, alfa stems are mainly constituted of cellulose fibres,

a renewable and biodegradable polymer. The chemical composition of Alfa stems, like any natural fibre, is mainly cellulose, hemicellulose and lignin [22-26]. In a much smaller proportion, they also contain extractible protein and some inorganic compounds [27]. The chemical extraction processes are needed to isolate the cellulose before use; the best known is the method of Kraft [28] which represents 90% of current extraction.
The composites based on PU and Alfa fibers, as most of composites reinforced with natural short fibers, can be used in the automotive industry such as covers, car doors panels and car roofs [29]. Recently, the use of the Alfa fibers in the field of medical textiles [30] and orthopedic applications [31] were also reported.
This work aims to develop new composite materials based on biosourced polyurethane. We report hereby on the synthesis and the characterization of the PU based on castor oil and composites based on the synthesized PU and Alfa cellulose fibers which are produced with different fibers ratios. The structures, thermal and mechanical properties of these composites are investigated.

2. Materials and methods

2.1. Apparatus

2.1. Materials and syntheses

2.1.1. Reagents

Alfa plants are collected from Jerada region in the east of Morocco in July 2013, the recommended time for harvesting Alfa plants. *Castor oil*, 4.4'diphenyl methylene diisocyanate (MDI), 1,3-propanediol and dibutyltin dilaurate (DBDTL) are purchased from Aldrich company. Chloroform (analysis grade), acetone (analysis grade), methanol (analysis grade) and diethyl ether are also supplied by Aldrich. As MDI could dimerize at room temperature, it is stored in a refrigerator at -10 °C. All reagents were used without prior purification.

2.1.2. Extraction of cellulosic fibers from Alfa stems

The extraction of cellulosic fibers is performed according to the procedures described in the literature [22, 23, 25, 28, 32]. The prepared fibers have a mean length of 0.6 mm and are dried and stored more than 1 week in a desiccator in presence of P_2O_5 to remove the maximum adsorbed water.

2.1.3. Polyurethane synthesis

Polyurethane was prepared by a two-step procedure. Castor oil (25g, 932 g.mol-1) and MDI (13.5g, 250 g.mol-1) were charged into a reactor equipped with mechanical stirring under inert atmosphere of nitrogen in the presence of DBTDL as catalyst at 0.02 *wt*% of *Castor oil*. The reaction is maintained at 90 °C for 2 h. After cooling, 1,3-propane diol (2g, 76g.mol^{-1}) was then added to the prepolymer. The mixture is again heated to 90 °C for 3 hours in dry nitrogen atmosphere. The product is obtained as yellow viscous oil.

2.1.4. Elaboration of Composites

Typical preparation was performed as follows: 5 g of PU and 10 ml of acetone were charged in a beaker equipped with magnetic stirrers. The mixture is stirred until dilute dispersions were obtained. Then, various amounts of cellulose fibers are incorporated. The mixture is stirred for 20 min and poured into Petri dishes. The solvent is removed by evaporation at room temperature for 24h and further drying is performed at 80°C for 48h. All the films were prepared by casting. The designation used for the prepared films are referenced in Table 1.

Table 1*:* Cellulose percentage and T_g of pure PU and different composites.

Samples	Cellulose (*wt* %)	T_g (°C)
PU100	0	-18.8
PU95	5	-16.4
PU90	10	-17.5
PU85	15	-11.7
PU80	20	-4.3
PU75	25	19.0
PU70	30	18.9
PU65	35	19.8

2.2. Techniques

2.2.1. Fourier Transform Infrared Spectroscopy (FTIR)
The FTIR spectra were recorded on a FTIR 8400 SHIMADZU in a range of 700-4000 cm^{-1} with a resolution of 4 cm^{-1}. Samples are in film form with 20 scans for each sample.

2.2.2. Differential Scanning Calorimetry (DSC)
DSC analyses were performed with a 204 F1 NETZSCH (Germany). Experiments are carried out under nitrogen. The temperature range of the first scan is from -80 to 250 °C, with a heating rate of 10 K.min-1, followed by a cooling at 20 K.min-1. A second scan is immediately performed with a heating rate of 10 K.min-1. The glass transition temperature was taken at the midpoint of heat capacity change after the second scan.

2.2.3. Thermogravimetric Analyses (TGA)
TGA measurements were performed on a TG 209 F3 NETZSCH 51 (Germany). About 15 mg of the samples was placed in a ceramic pan and heated from 30 to 600°C under nitrogen purge with a temperature ramp of 10 $K.min^{-1}$.

2.2.4. High strain mechanical properties
High strain mechanical tests are carried out with a "MTS Adamel Lhomargy-DY35XL (France)" machine equipped with a load of 500 N on dumbbell-shaped H3 samples (ISO 37, 34 mm length and 4 mm wide) at room temperature. The tensile speed was 10 mm/min. The Young's modulus, tensile strength, and elongation at break are calculated from stress-strain curves. For each sample, the mechanical properties are obtained from the average of tests on 10 specimens.

2.2.4. High strain mechanical properties
High strain mechanical tests are carried out with a "MTS Adamel Lhomargy-DY35XL (France)" machine equipped with a load of 500 N on dumbbell-shaped H3 samples (ISO 37, 34 mm length and 4 mm wide) at room temperature. The tensile speed was 10 mm/min. The Young's modulus, tensile strength, and elongation at break are calculated from stress-strain curves. For each sample, the mechanical properties are obtained from the average of tests on 10 specimens.

2.2.5. Scanning Electron Microscopy (SEM)
The measurements are carried out in a scanning electron microscope JEOL JSM-6460LA (Japan) equipped with an energy dispersive (Si-Li) X-ray spectrometer. The electron beam is incident on the specimen perpendicular to the surface and the measurements are performed under the following conditions: primary beam energy of 5 keV, working distance of 10 mm, take off angle of 30° and residual pressure in the specimen chamber below 10^{-5} Torr. All samples were broken at liquid nitrogen temperature and their facial fracture is analysed.

3. Results and discussion

3.1. Synthesis and characterization of PU and composites
Fig 1 illustrates the chemical structure of the castor oil. This is a triglyceride with three fatty acids linked by a glycerol unit. Approximately 90% of the fatty acid in the castor oil is ricinoleic acid which is a mono unsaturated with 18 carbons. Fatty acid presents a hydroxyl functional group at the 12^{th} carbon; this is a very rare property for a natural fatty acid and this is the main reason for the direct use of this oil as a hydroxyl-containing trifunctional monomer.
The organic matrix studied is a PU based on *castor oil*, MDI and 1,3-propanediol as a chain extender. To control the distribution of *castor oil* along polymer chain, segmented PU was synthesized in two steps. The first step consists of the reaction between *castor oil* and MDI. In the second step, obtained *PU* prepolymer is reacted with the chain extender, 1,3-propanediol. Fig.2 depicts the FTIR spectra of the *castor oil*, Alfa cellulose fiber, pure *PU* matrix (PU100) and composites with 15% (PU85) and 25% (PU75) of Alfa cellulose. The FTIR spectrum of PU100 shows the absorption bands characteristics of the N-H elongation, ester carbonyl group of the castor oil elongation, stretching vibration of C=O in urethane group, and out-of-plane distortion of N-H band, respectively at 3336, 1740, 1690 and 1530 cm^{-1} [33]. Moreover, the bands around 1240 cm^{-1} are assigned to the valence vibration of C-N and the deformation of N-H bonds of the urethane group [34].

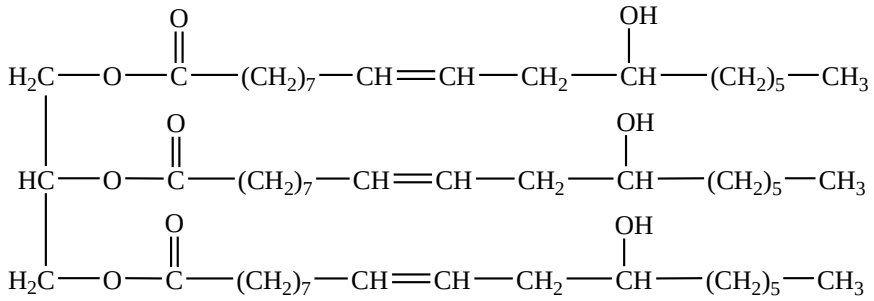

Figure 1: Structure of castor oil

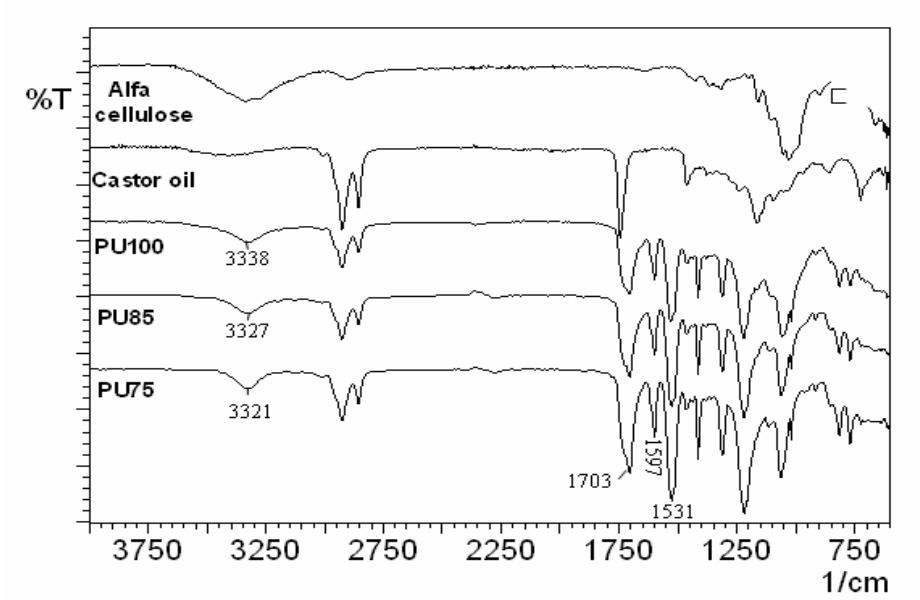

Figure 2: FTIR spectra of castor oil, pure PU and composites PU85 and PU75

In the FTIR spectra of the composites, the band characteristic of the stretching vibration of N-H bonds at 3338 cm^{-1} is shifted to 3327 cm^{-1} and 3321 cm^{-1} for PU85 and PU75, respectively. In addition, this band is larger in the composites compared to the one of the pure PU.

These results could be explained by the presence of hydrogen bonds between the N-H bonds of the PU matrix and the O-H groups of cellulose. There is also an intensification of the valence vibration band of C=O in urethane group at 1690 cm^{-1} and the band at 1031 cm^{-1} due to the stretching vibration of C-O bonds in the alcohol and ether functions of the cellulose.

When comparing the bands at 1690 cm^{-1} for the *PU* and the composites, one can clearly observe a significant intensification of this band in the composites. This could be explained by the presence of a hydrogen bonds between the C=O groups of the *castor oil* and O-H groups of the cellulose. Another parameter that could contribute to the intensification of the band at 1690 cm^{-1} is the formation of urethane groups from a slight residual NCO function and the OH of cellulose. All these results show clearly the existence of secondary interactions and/or covalent bonds between the matrix and cellulose fiber.

3.2. Composites properties characterizations

3.2.1. Thermal properties

Figure 3 reports the DSC thermograms of the PU and the composites. The values of *Tg* of all samples are reported in Table 1. Worthy to notice that the increase of the Alfa cellulose content leads to an increase in the *Tg*. In fact, *Tg* shifts from - 18.8°C for the pure PU to 19.8 °C for PU65 (35% of cellulose). In general, the increase in the *Tg* value of the PU flexible segments indicates the presence of strong interactions between the matrix and reinforcement via the hydrogen and/or covalent bonding.

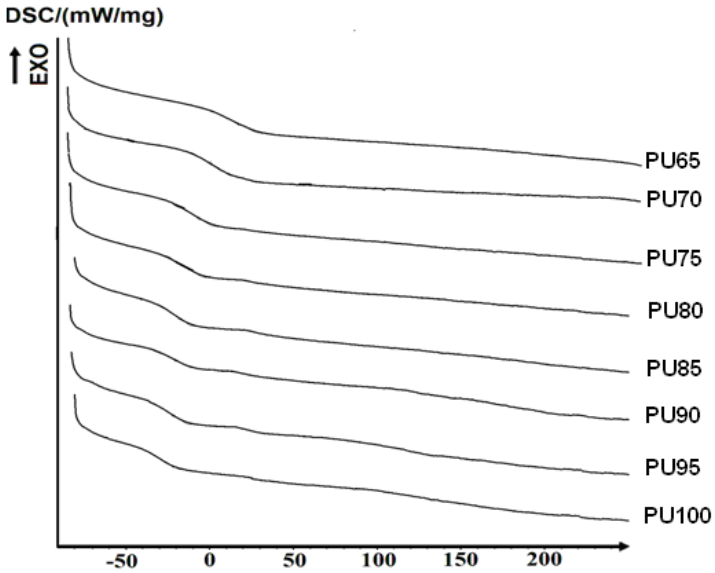

Figure 3: Second scan DSC thermograms of different composites

These results are in good agreement with FTIR analysis results which showed strong interaction between the PU and the fibers. However, and at this stage of study we cannot explain with certainty the origin of the small exothermic peak at 25 °C. According to literature, it could be attributed to the crystallization of the hard segments of the PU [3, 9, 35].
TGA curves, which show the effect of the fiber content, are presented in Fig.4. The first weight lost observed at lower temperature, between 25 and 200 °C, could be attributed to the water molecules evaporation.

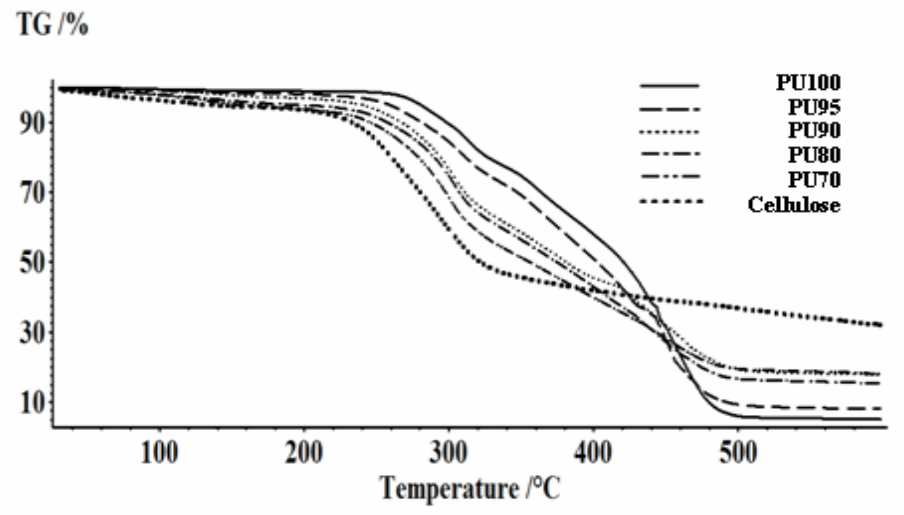

Figure 4: TGA thermograms of pure PU and different composites

The fraction of weight lost in this range increases with the cellulose fibers content. In fact, Cellulose fibers are hydrophilic material and the resulting composites becomes increasingly hydrophilic when the fraction of cellulose fibers increases. From this analysis one can clearly see that the neat cellulose fibers are the less thermally stable materials and the PU is the most stable one. The composites have intermediate thermal stability. In fact, the cellulose fibers thermal degradation starts at around 200 °C and this of the pure PU starts at 265 °C. The composites materials show theirs starting thermal degradation temperature between these two temperatures. On the other hand, at 50% of mass loss, the degradation temperature of the composites decrease with the increase of the incorporated cellulose percentage (Table 2), it shifts from 420 °C for PU100 to 355 °C for PU70.

Table 2: Thermogravimetrical characteristics of pure PU, cellulose and different composites.

Samples	Temperature at 30% of mass loss	Temperature at 50% of mass loss	Percentage of mass loss at 280°C
PU100	363	420	5.2
PU95	346	402	9.4
PU90	311	380	13.7
PU80	306	372	15.4
PU70	298	355	19.6
Cellulose	280	320	28.8

Similarly, the temperature at 30% of mass loss shifts from 363°C (PU 100) to 298 °C (PU70). Furthermore, at 280 °C, the mass loss increases with cellulose content, 5.2% for PU100 and 19.6% for PU70. Meanwhile at high temperature (beyond 400 °C) the residual mass increases as the percentage of cellulose rises (Fig. 4). This residual mass results from the carbonization of the cellulose fibers.

3.2.2. Morphological properties

The image of the fractured surface of PU100 (Fig. 5a), PU90 (Fig. 5b), PU70 (Fig. 5c) and PU60 (Fig. 5d) are recorded and analyzed. PU100 matrix presents a homogeneous morphology.

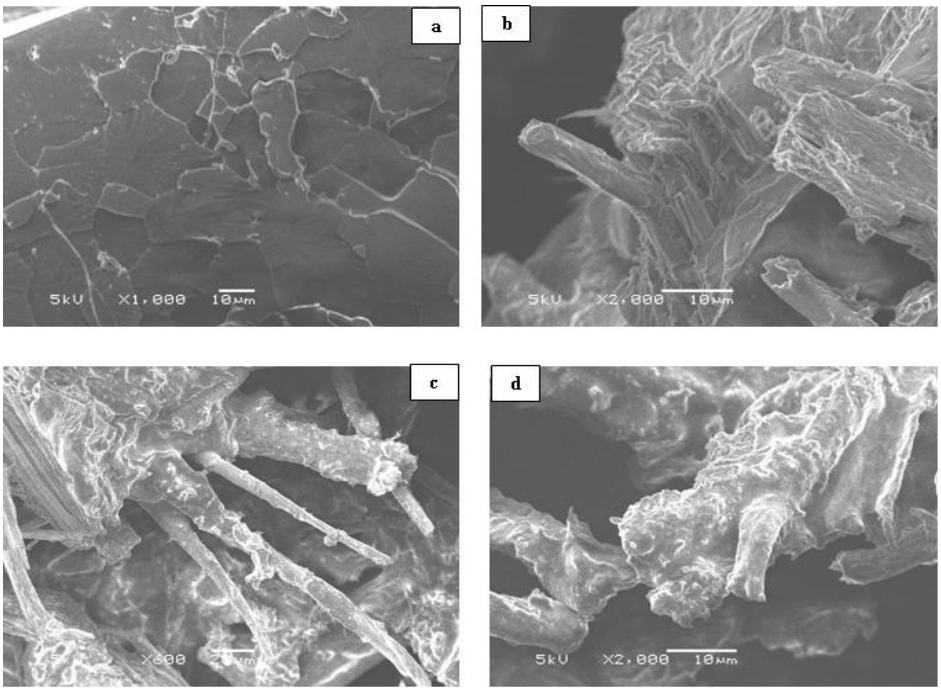

Figure 5: Facial fracture images (a): PU100, (b): PU70, (c): PU90, and (d): PU60

Alfa cellulose fibres can be clearly seen in composite samples. The pulled out fibers are covered with the polymer [Figs. 5(c, d)]. This reflects a good adhesion at the fiber-matrix interface resulting from hydrogen bonding and possible covalent bonding between two phases, as reported previously in FTIR and DSC results.

3.2.3. High strain Mechanical properties

The properties of the composites reinforced by natural fibres depend on different parameters, such as fiber volume fraction, fiber-matrix adherence, fibers length and orientation. Various studies were conducted on the natural fiber-based composites including the effect of the fibers content, fiber treatments, on the mechanical properties [36, 37]. Other aspects of the prediction of modulus and resistance behavior are also studied using some predefined templates for bi-phased systems and a comparison with experimental data is reported [38]. The

properties of the matrix and fiber play an important role in the enhancement of composite mechanical properties. Indeed, the tensile strength is more sensitive to the properties of matrix whereas the Young's modulus depends on the properties of the fibres [26, 38]. To improve tensile strength, a good interface, low concentration and good orientation of fibres are recommended. Meanwhile the wetting of fiber in the matrix and the high fiber content determine the resistance modulus. The matrix/fiber ratio is very important when determining fracture properties. In the composites reinforced by short fibres, the critical length of fiber is required to develop key conditions for obtaining optimal properties of composites. Fibres of a length less than the critical value are not successful due to the rupture of bonds at the interface under low loads. In the opposite case, fibres that are longer than the critical length can be deformed under loads leading to high strength composites. Oksman et al. have noted that many dispersed small fibres generally increase resistance properties, whereas length fibres improve the mechanical properties [39]. Furthermore, this is confirmed by Sanadi et al identified that small fibres improve rigidity, while large fibres improve the tensile strength [40].
To get a good impact resistance, an optimal fiber-matrix interaction is essential. The degree of fiber adhesion and the energy absorption mechanism represent examples of the parameters that can influence the impact resistance of composites enhanced with short fibres. The mechanical properties increase linearly with the composition according to the rule of mixtures. However, this linear dependence of the fiber content is no longer valid for large fiber percentage and could be probably due to the lack of total fiber immersion in the polymer matrix in the latter case.
The stress-strain curves of the composites studied in this work are showed in Fig. 6a and the numerical data are collected in Table 3.

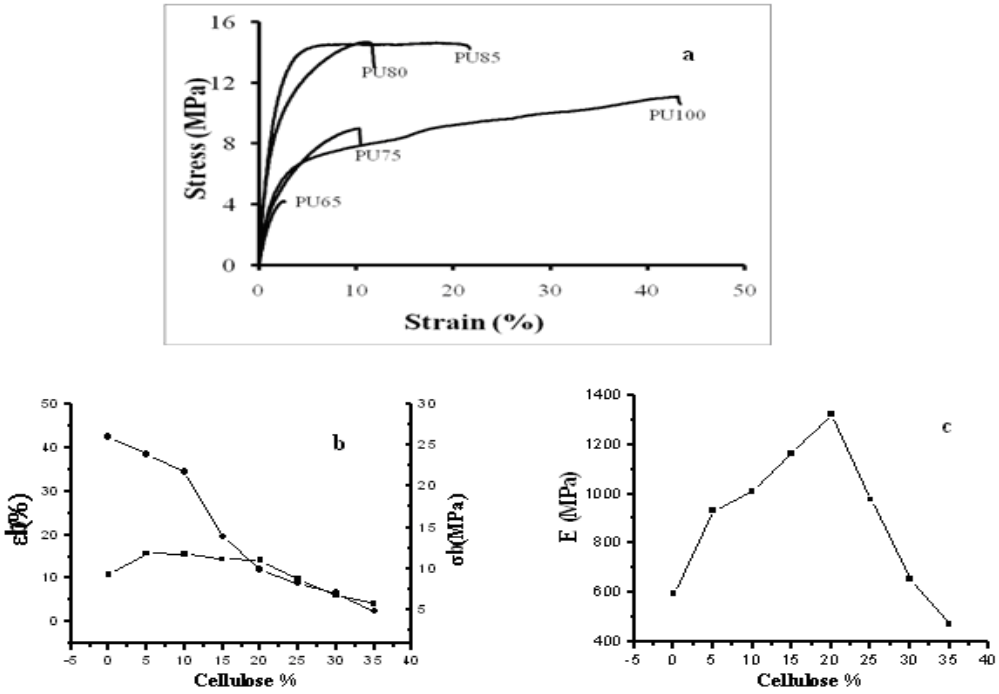

Figure 6: Mechanical properties of the composites (a): Stress-strain curves of pure PU and various composites; (b): Deformation (●) and stress (■) at break versus cellulose percentage ; (c): Young Modulus versus cellulose percentage

The results show a decrease in strain at break and a marked improvement in the Young's modulus when the cellulose content in the composites increases up to 20%. Beyond this value, the modulus decreases. The modulus increases by 56.5% for the composite PU95 where the amount of incorporated cellulose is 5 *wt* %, and by 70% for a cellulose content of 10 *wt*% (PU90). The cellulose contents of 15 *wt*% and 20 *wt*% lead to a modulus increase of 95% and 122%, respectively. Figure 6b&c shows clearly the dependence of mechanical properties on cellulose content. Indeed, the Young's modulus reaches a maximum value with 20% of cellulose and has the lowest value with 35%. Furthermore, the stress at break depends to some extent on cellulose content. It decreases sharply beyond the fibers content of 20 *wt*%. However, it is very low with cellulose content

of more than 35%. The reduction of the mechanical properties at fibers contents higher than 20 *wt*% is certainly due to a bad dispersion of the fibers within the PU matrix. This results in the formation of aggregates that become weakness point of the composites.

Table 3: Mechanical properties of pure PU and different composites.

Samples	Deformation at break (%)	Young's modulus (MPa)	Stress at break (MPa)
PU100	42.5 ± 19.5	595 ± 24	10.9 ± 1.7
PU95	38.5 ± 9	931.4 ± 30.6	15.7 ± 1.6
PU90	34.5 ± 6.5	1010.2 ± 59.5	15.6 ± 1.4
PU85	19.5 ± 11.1	1162.8 ± 106.1	14.4 ± 1.4
PU80	11.9 ± 3.8	1321.2 ± 81.1	14.0 ± 1.3
PU75	11.8 ± 1.8	976.7 ± 96.1	9.7 ± 0.9
PU70	6.6 ± 2.2	654 ± 56.9	6.0 ± 1.1
PU65	2.5 ± 0.4	392.5 ± 28.7	4.2 ± 0.9

Many reports in literature emphasize the difficulties that appear when manufacturing natural fibers based composites with high fibers contents. It is actually quite rare to find reinforced polymers containing a percentage of wood superior to 50-60%, at which many difficulties appear in the molding and these difficulties increase in the order: compression, extrusion, injection. Thus, Klason et al. [41] observed that beyond 50%, the material becomes rough and presents surface cracks. A large amount of fibres also creates problems when mixing components. Moreover, the increase in the fibres content can cause a number of drawbacks, notably the hygroscopic properties and degradability of composites as well as their low elongation and low impact resistance.

Conclusion

Composites are prepared with different percentage of the *Alfa* cellulose fibres and *Castor oil* based PU. The results of all characterization techniques show that both thermal and mechanical properties of the composite are improved by the presence of the *Alfa* cellulose fibres. Moreover, this improvement shows a linear dependence with the rate of the incorporated fiber up to 20%. Beyond this value, the mechanical properties of the composites decline. However, the facial rupture images illustrate a good interface because of the hydrogen bonding and possible covalent bonding between the fiber and the matrix. To enhance further mechanical properties and to increase the fiber content, a fiber surface treatment should be used to favor the matrix-fiber interaction at the interface. Likewise, an improvement in processing would be desirable to homogeneously disperse fibers in the matrix.

Acknowledgements-The authors gratefully thank the AUF (Project MeRSI – Ref : 6313PS006) and the CNRST (Morocco) for their financial support of this work.

References

1. Belgacem M. N., Gandini A.: *Monomers, Polymers and Composites from renewable Resources*. Elsevier. (2008).
2 Gandini A. *Macromolecules*. 41 (2008) 9491.
3 Merlini C., Barra G. M. O., Schmitz D. P. , Ramôa S. D.A.S, Silveira A., Araujo T. M., Pegoretti A., *Polym. Test.* 38 (2014) 18.
4 Pfister D. P., Xia Y., Larock RC. *ChemSus Chem*, 4 (2011) 703.
5 Luo X., Mohanty A., Misra M. *Indus. Crops Prodt*, 47 (2013) 13.
6 Stemmelen M., Pessel F., Lapinte V., Caillol S., Habas J. P., Robin J.J. *J. Polym. Sci. Part A: Polym. Chem.* 49 (2011) 2434.
7 Yari A., Yeganeh H., Bakhshi H., Gharibi R., *J. Biomed. Mater. Res. A*. 102 (2014) 84.
8 Zhang L., Zhang M., Hu L., Zhou Y. *Indus. Crops Prodt*. 52 (2014) 380.

9 Miléo P. C., De Moraes Rocha G. J., Gonçalves A. R. *Adv. Mater. Res.* 415-417 (2012) 1103.
10 Ristić I. S., Simendić J. B., Krakovsky I., Valentova H., Radicević R., Cakić S., Nikolić N. *Mater. Chem. Phys.* 132 (2012) 74.
11 Abdul Nasir A. A., Azmi A. I., Khalil A. N. M., *Procedia Manuf.* 2 (2015) 97.
12 Arbelaiz A., Cantero G., Fernandez B., Mondragon I., Ganãn P., Kenny J. M. *Polym. Compos.* 26 (2005) 324.
13 Stamboulis A., Baillie C., Schulz E. *Angew. Makromol. Chem.* 272 (1999) 117.
14 Eichhorn S. J., Young R. J. *Compos. Sci. Technol*. 64 (2004) 767.
15 Li Y., Mai Y. W., Ye L. *Compos. Sci. Technol*. 60 (2000) 2037.
16 Torres F. G., Cubillas M. L. *Polym. Test.* 24 (2005) 694.
17 Alemdar A., Sain M. *Bioresour. Technol.* 99 (2008) 1664.
18 Angelini L. G., Lazzeri A., Levita G., Fontanelli D., Bozzi C. *Indus. Crops Prodt*. 11 (2000) 145.
19 Shinoj S., Visvanathan R., *Panigrahic* S., Kochubabu M. *Indus. Crops Prodt.* 33 (2011) 7.
20 Auad M. L., Richardson T., Hicks M., Mosiewicki M. A., Aranguren M. I., Marcovich N. E. *Polym. Int.* 61 (2012) 321.
21 Reis J. M. L., Motta E. P. *Compos. Struct*, 111 (2014) 468.
22 Ben Brahim S., Ben Cheikh R. *Compos. Sci. Technol*. **67** (2007) 140.
23 Bessadok A., Marais S., Gouanve F., Colasse L., Zimmerlin I., Metayer M. *Compos. Sci. Technol*, **67** (2007) 685.
24 Abdul Khalil H.P.S., Bhat A.H., Ireana A.F. Yusra. *Carbohydr. Polym*. 87 (2012) 963.
25 Maafi E. M., Malek F., Tighzert L., Dony P. *J. Polym. Env.*18 (2010) 638
26 Paiva M. C., Ammar I., Campos A. R., Ben Cheikh R., Cunha A. M. *Compos. Sci. Technol.* 67 (2007), 1132.
27 Bohli N., Perwuelz A., Ben Cheikh R., Baklouti M. *J. Appl. Polym. Sci*. 110 (2008) 3322.
28 Krassig H., Schurz J., Steadman R. G., Schliefer K., Albrecht W., Mohring M., Schlosser H.: Cellulose: Ullmann's Encyclopedia of Industrial Chemistry. **7**, (2012).
29 Zaleha M., Mahzan S., Maizlinda Izwana I. *App. Mech. Mater*. 229-231 (2012) 276.
30 Sayeb S., Marzoug I., Hassen M. B., Sakli F., Rodesli S. *J. Text. I.* 101 (2010) 19.
31 Vermeulen B., Ben Youssif Y., Perwuelz A., Legrand X., Vroman P., Ben Cheikh R. *Revue des Composites et des Matériaux Avancés*, Ed Lavoisier (Paris). 18 (2008) 139.
32 Zuluaga R., Putaux J. L., Cruz J., Vélez J., Mondragon I., Gañan P. *Carbohydr. Polym*. 76 (2009), 51.
33 Sun J. X., Sun X. F., Zhao H., Sun R. C. *Polym. Degrad. Stab.* 84 (2004) 331.
34 Yeganeh H., Hojati-Talemi P. *Polym. Degrad. Stab.* 92 (2007) 480.
35 Bendahou A., Dufresne A., Kaddami H., Habibi Y. *Carbohydr. Polym.* 68 (2007) 601.
36 Puglia D., Tomassucci A., Kenny J.M. *Polym. Adv. Technol.* 14 (2003) 749.
37 Saheb D. N., Jog J. P. *Adv. Polym. Tech.* 18(4) (1999) 351.
38 Miléo P. C., Mulinari D. R., Baptista C. A. R. P., Rocha G. J. M., Gonçalves A. R. *Procedia. Eng.* 10 (2011) 2068.
39 Imed Miraoui I., Hassis H. *Phys. Procedia.*25 (2012) 130.
40 Jayaramudu J., Siva Mohan Reddy G., Varaprasad K., Sadiku E.R., Sinha Ray S., Varada Rajulu A. *Carbohydr. Polym.*, 93 (2013) 622.
41 Klason C., Kubat J., Stromval H.E. *Int. J. Polym. Mater. Po.* 10 (1984) 159.